

Bifurcation Phenomena of Switched Dynamical Systems based on the Boost Converters with Photovoltaic Input

Maho Wakabayashi and Toshimichi Saito

Department of Electrical and Electronics Engineering, HOSEI University
 Koganei-shi, Tokyo, 184-8584 Japan, tsaito@hosei.ac.jp

Abstract—This paper studies bifurcation phenomena of boost converters with photovoltaic input and the average power. In the system, the photovoltaic input is simplified into a piecewise linear current-controlled voltage source (CCVS). The switching rule has nonlinear cycle. The system dynamics is described by simple piecewise linear equation and the 1D return map can be derived. The map describes switching phase and makes precise analysis possible. Typical periodic/chaotic phenomena related bifurcation phenomena are demonstrated and circuit experiment. Also, we will study about parallel converter.

I. INTRODUCTION

The switched dynamical system (SDS [1]-[3]) consists of continuous subsystems connected by a discrete switching rule. Depending on the rule and parameters, the SDSs can exhibit various periodic/chaotic phenomena and related bifurcation phenomena. As typical and concrete examples of the SDSs in engineering systems, switching power converters and A/D converters have been studied. This paper studies stability and basic bifurcation phenomena of a simple SDS based on the boost converter with photovoltaic (PV) input. Power converters of the PV input has been attracted a lot of attention as efficient renewable energy systems [4]-[6]. In our system, the PV input corresponds to a solar cell. The PV input is applied to the dc-dc boost converter with current mode control switching.

In order to simplify the analysis, we replace the smooth voltage-current characteristics of the PV with two-segment piecewise linear characteristics [7] [8]. Also, assuming a high frequency operation, we replace the output load with a constant voltage source [9]. Deriving one-dimensional return map of a state variable at every switching instants, we can analyze stability of fundamental periodic waveforms and their power characteristics precisely. Especially, we have clarified that unstable periodic orbit can have larger average power than stable periodic orbit.

II. CIRCUIT AND SWITCHING RULE

Figure. 1 shows the simplified model of the boost converter with photovoltaic characteristic. Here we derive a dimensionless state equation of the simple SDS based on the boost converter with PV input. First, we simplify the PV input by

2-segment piecewise linear current-controlled voltage source (CCVS):

$$V_i(i) = \begin{cases} -\gamma_a(i - I_P) + V_P & \text{for } i \leq I_P \\ -\gamma_b(i - I_P) + V_P & \text{for } i > I_P \end{cases} \quad (1)$$

The boost converter has a switch S and a diode D . They can be either of the following 2 states:

- State 1: S conducting and D blocking
- State 2: S blocking and D conducting.

The fig. 3 is circuit model, boost converter. We replace the part of photovoltaic input by constant voltage source and two resistances. Also, we replace a capacitor and resistance by constant voltage source. Assuming that time constant is much larger than the clock period T , we can simplify the output load into a constant-voltage source V_o . The switching rule is defined by

$$\begin{aligned} \text{State 1} &\rightarrow \text{State 2 at } t = nT \text{ and } i > J_- \\ \text{State 2} &\rightarrow \text{State 1 when } i = J_- \end{aligned} \quad (2)$$

where J_- is the lower threshold. Figure 3 illustrates the switching rule.

Let the system be State 1. If a clock pulse arrives at time $t = nt$ then State 1 is switched into State 2. If an inductor current i reaches the lower threshold then State 2 is switched into State 1. Repeating such operations, the system can exhibit

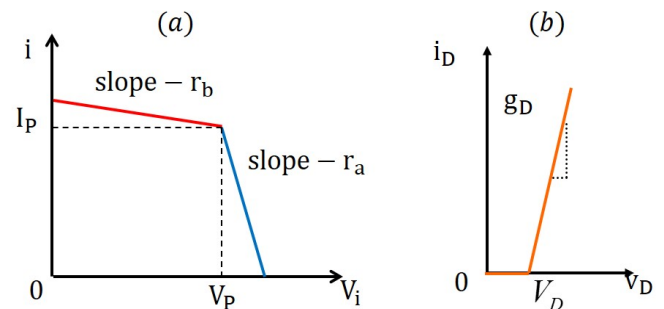


Fig. 1. (a) the simplified photovoltaic characteristic, (b) a diode characteristic

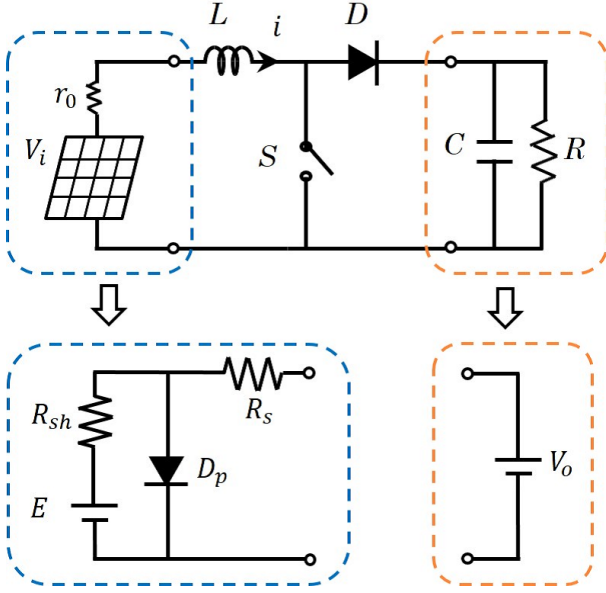


Fig. 2. boost converter

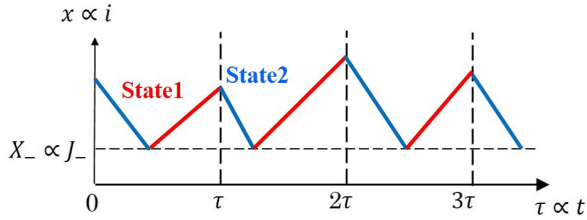


Fig. 3. Switching Rule

a variety of periodic /chaotic phenomena. The circuit dynamics is described by

$$L \frac{di}{dt} = \begin{cases} V_i(i) & \text{for State 1} \\ V_i(i) - V_o & \text{for State 2} \end{cases} \quad (3)$$

Using the following dimensionless variables and parameters,

$$\begin{aligned} \tau &= \frac{t}{T}, \quad x = \frac{i}{I_P}, \quad y(x) = \frac{T}{LI_P} V_i(I_P x), \quad \alpha = \frac{\gamma_a I_P}{V_P} \\ \beta &= \frac{\gamma_b I_P}{V_P}, \quad q = \frac{V_o}{V_P}, \quad \gamma = \frac{TV_P}{LI_P}, \quad X_- = \frac{J_-}{I_P}, \end{aligned} \quad (4)$$

Eqs. (1) and (3) are transformed into

$$\frac{dx}{d\tau} = \begin{cases} \gamma y(x) & \text{for State 1} \\ \gamma(y(x) - q) & \text{for State 2} \end{cases} \quad (5)$$

$$y(x) = \begin{cases} -\alpha(x-1) + 1 & \text{for } x \leq 1 \\ -\beta(x-1) + 1 & \text{for } x > 1 \end{cases} \quad (6)$$

SW Rule:

$$\begin{aligned} \text{State 1} &\rightarrow \text{State 2: at } \tau = n \text{ and } x > X_- \\ \text{State 2} &\rightarrow \text{State 1: when } x = X_- \end{aligned} \quad (7)$$

The dimensionless 5 parameters can be classified into two categories: (α, β, q) , which characterizes "solar cell and load", and (γ, X_-) , which characterizes "switching control". γ is

parameter which relates temperature. The exact piece-wise solution is given by

State 1:

$$\begin{cases} x(\tau) = (x_0 - x_{e1})e^{-\gamma\alpha(\tau-\tau_0)} + x_{e1} & \text{for } x \leq 1 \\ x(\tau) = (x_0 - x_{e2})e^{-\gamma\beta(\tau-\tau_0)} + x_{e2} & \text{for } x > 1 \end{cases} \quad (8)$$

State 2:

$$\begin{cases} x(\tau) = (x_0 - x_{e3})e^{-\gamma\alpha(\tau-\tau_0)} + x_{e3} & \text{for } x \leq 1 \\ x(\tau) = (x_0 - x_{e4})e^{-\gamma\beta(\tau-\tau_0)} + x_{e4} & \text{for } x > 1 \end{cases} \quad (9)$$

$$\begin{aligned} x_{e1} &= 1 + 1/\alpha, \quad x_{e2} = 1 + 1/\beta \\ x_{e3} &= q/\alpha - 1 - 1/\alpha, \quad x_{e4} = q/\beta - 1 - 1/\beta \end{aligned}$$

where (τ_0, x_0) indicates an initial condition, Using these equations, we can calculate waveform precisely. In this paper we select *gamma* as a control parameter. This parameter can represent influence of temperature. The other parameters are fixed:

$$\alpha = 1.0, \quad \beta = 5, \quad q = 1.5, \quad X_- = 0.7.$$

In order to consider the power characteristics, we define the dimensionless and average powers;

$$P_A = \frac{1}{N_P} \int_0^{N_P} P_i(\tau) d\tau, \quad P_i(\tau) = x(\tau)y(\tau), \quad (10)$$

Figure. 4 shows the instantaneous and average powers. We calculate each stable PEOs average powers and unstable powers. It should be noted that the average power of unstable PEO (Fig. 4 (b) and (c)) are larger than that of stable PEOs in Fig. 4 (b') and (c').

III. RETURN MAP AND STABILITY

In order to analyze the stability and power characteristics, we define the return map. Let x_n be the dimensionless current when the n -th clock arrives and the SDS is State 2 where x decreases. Since x_{n+1} is determined by x_n as shown in Fig. 5, we can define a return map $x_{n+1} = F(x_n)$. The return map can be described exactly using the exact piece-wise solutions. Figure 6 shows examples of the return map corresponding to Fig. 4. The return map in Fig. 6 (a) has a stable fixed point that corresponds to stable PEO in Fig. 4 (a). As *gamma* decreases, this fixed point becomes unstable via the period doubling bifurcation and return map has stable PEO with period 2 as shown in Fig. 6 (b). The unstable fixed point and stable PEO with period 2 is corresponding to waveforms in Fig. 4 (b) and (b'), respectively.

Figure. 7 (a) shows one-parameter Stability diagram for γ . We can see that the stable orbit changes to unstable orbit when γ decrease to 1.3.

IV. CONCLUSIONS

This paper studies a simple SDS based on the boost converter with photovoltaic input. Applying the piecewise linear simplification and mapping procedure, stability and power characteristics have been analyzed precisely. Especially, we

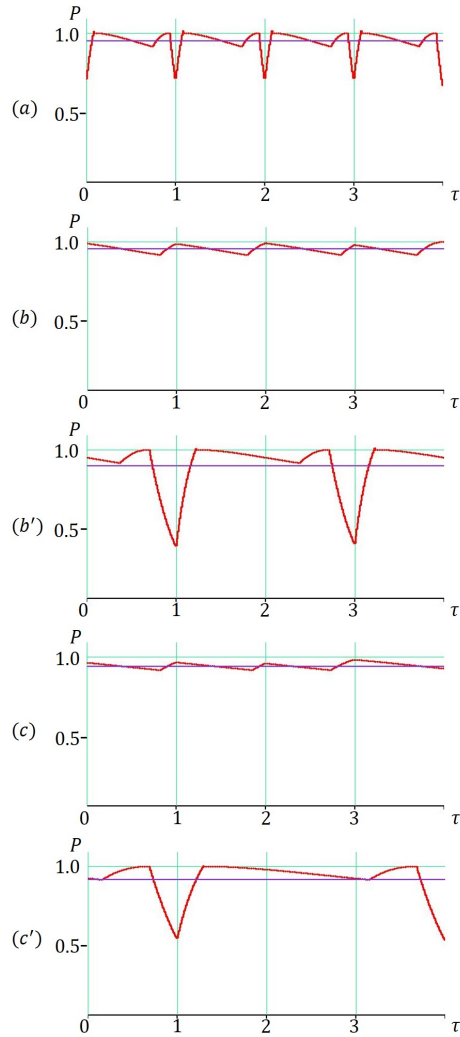


Fig. 4. Instantaneous power and average power P_a . (a) Stable PEO with period 1 for $\gamma \doteq 1.4$, $P_a \doteq 0.945$. (b) Unstable PEO with period 2 for $\gamma \doteq 0.8$, $P_a \doteq 0.950$. (b') Stable PEO with period 2 for $\gamma \doteq 0.8$, $P_a \doteq 0.888$. (c) Unstable PEO with period 3 for $\gamma \doteq 0.5$, $P_a \doteq 0.936$. (c') Stable PEO with period 3 for $\gamma \doteq 0.5$, $P_a \doteq 0.911$.

have clarified that unstable periodic orbit can have larger average power than stable periodic orbit. Future problems include fabrication of a simple test circuit, laboratory experiments, and analysis of bifurcation phenomena.

REFERENCES

- [1] S. Banerjee and G. C. Verghese, eds., *Nonlinear Phenomena in Power Electronics: Attractors, Bifurcations, Chaos, and Nonlinear Control*, IEEE Press, 2001.
- [2] C. K. Tse and M. di Bernardo, Complex behavior in switching power converters, *Proc. IEEE*, 90, pp. 768-781, 2002.
- [3] J. H. B. Deane, P. Ashwin, D. C. Hamill and D. J. Jeffries, Calculation of the periodic spectral components in a chaotic dc-dc converter, *IEEE Trans. Circuits Syst. I*, 46, 11, pp. 1313-1319, 1999.
- [4] H. S.-H. Chung, K. K. Tse, S. Y. Ron Hui, C. M. Mok and M. T. Ho, A Novel Maximum Power Point Tracking Technique for Solar Panels Using a SEPIC or Cuk Converter, *IEEE Trans. Power Electron.*, 18, 3, pp. 717-724, 2003.

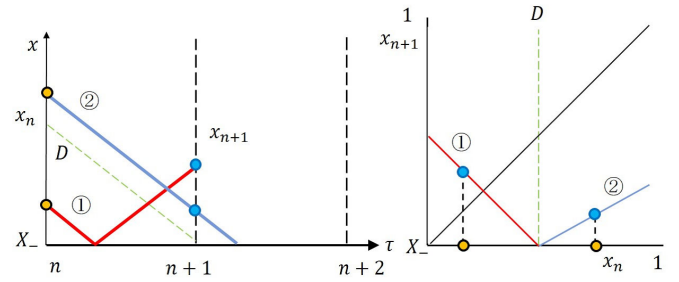


Fig. 5. Definition of return map

- [5] N. D. Benavides and P. L. Chapman, Modeling the Effect of Voltage Ripple on the Power Output of Photovoltaic Modules, *IEEE Trans. Ind. Electron.*, 55, 7, pp. 2638-2643, 2008.
- [6] D. Sera, R. Teodorescu, J. Hantschel and M. Knoll, Optimized Maximum Power Point Tracker for Fast-Changing Environmental Conditions, *IEEE Trans. Ind. Electron.*, 55, 7, pp. 2629-2637, 2008.
- [7] D. Kimura and T. Saito, A Simple Switched Dynamical System based on Photovoltaic Systems, *Proc. of NOLTA*, pp. 487-490, 2009.
- [8] H. Matsushita and T. Saito, Application of Particle Swarm Optimization to Parameter Search in Dynamical Systems, *NOLTA, IEICE, E94-N*, 10, pp. 458-471, 2011.
- [9] T. Saito, T. Kabe, Y. Ishikawa, Y. Matsuoka and H. Torikai, Piecewise constant switched dynamical systems in power electronics, *Int'l J. of Bifurcation and Chaos*, 17, 10, pp. 3373-3386, 2007.

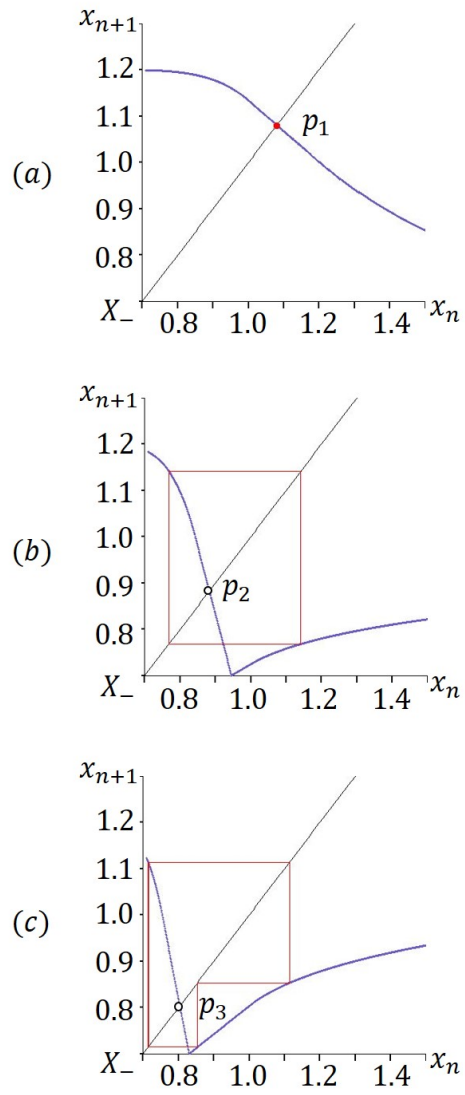


Fig. 6. Examples of the return map. (a) $\gamma \doteq 1.4$ (b) $\gamma \doteq 0.8$ (c) $\gamma \doteq 0.5$.

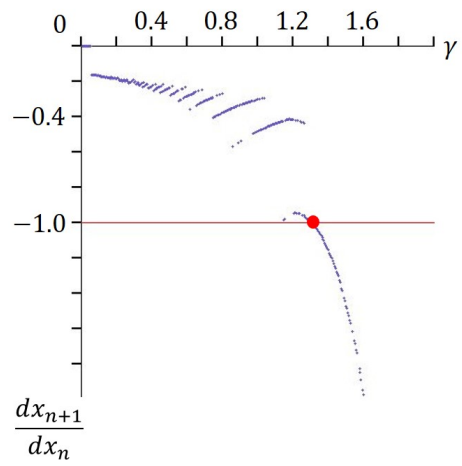


Fig. 7. Stability by γ and β